Structural and optical characterization of type-II InAs/InAs1−xSbx superlattices grown by metalorganic chemical vapor deposition

E. H. Steenbergen, Y. Huang, J.-H. Ryou, L. Ouyang, J.-J. Li, D. J. Smith, R. D. Dupuis, and Y.-H. Zhang

Citation: Applied Physics Letters **99**, 071111 (2011); doi: 10.1063/1.3625429
View online: http://dx.doi.org/10.1063/1.3625429
View Table of Contents: http://scitation.aip.org/content/aip/journal/apl/99/7?ver=pdfcov
Published by the AIP Publishing

Articles you may be interested in

Impact of substrate temperature on the structural and optical properties of strain-balanced InAs/InAsSb type-II superlattices grown by molecular beam epitaxy
Appl. Phys. Lett. **102**, 071903 (2013); 10.1063/1.4793231

Structural properties of InAs/InAs1–xSbx type-II superlattices grown by molecular beam epitaxy
J. Vac. Sci. Technol. B **30**, 02B106 (2012); 10.1116/1.3672026

Strain-balanced InAs/GaSb type-II superlattice structures and photodiodes grown on InAs substrates by metalorganic chemical vapor deposition
Appl. Phys. Lett. **99**, 011109 (2011); 10.1063/1.3609240

InAs/GaSb type-II superlattice structures and photodiodes grown by metalorganic chemical vapor deposition
Appl. Phys. Lett. **96**, 251107 (2010); 10.1063/1.3456386

Characteristics of Ga As N/Ga As Sb type-II quantum wells grown by metalorganic vapor phase epitaxy on GaAs substrates
J. Appl. Phys. **98**, 123525 (2005); 10.1063/1.2148620

Confidently measure down to 0.01 fA and up to 10 PΩ
Keysight B2980A Series Picoammeters/Electrometers
View video demo›

This article is copyrighted as indicated in the article. Reuse of AIP content is subject to the terms at: http://scitation.aip.org/termsconditions. Downloaded to IP: 209.147.144.24 On: Thu, 05 Feb 2015 17:49:47

Structural and optical characterization of type-II $InAs/InAs_{1-x}Sb_x$ superlattices grown by metalorganic chemical vapor deposition

E. H. Steenbergen,[1,2] Y. Huang,[3] J.-H. Ryou,[3] L. Ouyang,[1,4] J.-J. Li,[1,2] D. J. Smith,[1,4] R. D. Dupuis,[3] and Y.-H. Zhang[1,2,a)]

[1]*Center for Photonics Innovation, Arizona State University, Tempe, Arizona 85287, USA*
[2]*School of Electrical, Computer and Energy Engineering, Arizona State University, Tempe, Arizona 85287, USA*
[3]*Center for Compound Semiconductors and School of Electrical and Computer Engineering, Georgia Institute of Technology, Atlanta, Georgia 30332-0250, USA*
[4]*Department of Physics, Arizona State University, Tempe, Arizona 85287, USA*

(Received 9 June 2011; accepted 25 July 2011; published online 18 August 2011)

Strain-balanced type-II $InAs/InAs_{1-x}Sb_x$ superlattices with various compositions (x = 0.22, 0.23, 0.37) and different layer thicknesses (t_{InAs} = 7 nm, t_{InAsSb} = 3.3, 2.3, 2.0 nm, respectively) have been grown by metalorganic chemical vapor deposition on GaSb substrates. X-ray diffraction revealed narrow satellite peaks (full-width-half-maximum of <100 arc sec), indicative of uniform superlattice periodicity and excellent crystallinity, which was also corroborated by cross-sectional transmission electron microscopy observations. Despite relaxation, low-temperature photoluminescence measurements showed peaks at 6.7 μm and 5.8 μm, while photoconductance results showed strong spectral response up to 200 K, when the photoresponse onset was 8.6 μm. © *2011 American Institute of Physics*. [doi:10.1063/1.3625429]

Type-II superlattices (SLs) have been extensively investigated for infrared applications since their initial proposal[1,2] and the first InAs/GaSb SL experimental demonstration.[3] These SLs enable energy transitions that are smaller than the bandgaps of the constituent materials, even far beyond the smallest bandgap of any unstrained bulk III-V material, which is 9 μm for $InAs_{0.39}Sb_{0.61}$ at 77 K.[4] The following advantages make III-V SL photodetectors viable alternatives for expensive HgCdTe infrared detectors: greater control of the alloy composition and layer thickness, resulting in more uniform materials and cutoff wavelengths;[5] stronger bonds and structural stability;[6] less expensive, closely lattice-matched substrates, i.e., GaSb;[7] mature III-V growth and processing technology;[7] lower band-to-band tunneling due to larger electron effective mass;[5] and strain engineering in combination with larger effective masses reducing Auger recombination.[5,7–9] Recently, mid and long-wavelength infrared (LWIR) focal plane arrays using InAs/(In)GaSb SLs have been demonstrated by several groups.[10–14] The performance of InAs/(In)GaSb SLs is approaching that of HgCdTe,[7] but the minority carrier lifetime of the InAs/(In)GaSb SLs is limited by Shockley-Read-Hall (SRH) recombination and the background carrier concentration is considerably higher than that of HgCdTe.[15]

$InAs/InAs_{1-x}Sb_x$ SLs represent another alternative for infrared laser[16] and detector applications due to possible lower SRH recombination,[17] and the absence of gallium, which simplifies the SL interfaces and the growth process.[18] An ideal theoretical comparison of a 10-μm $InAs/InAs_{1-x}Sb_x$ SL with an 11-μm $InAs/In_xGa_{1-x}Sb$ SL on GaSb substrates revealed that the performance of the $InAs/In_xGa_{1-x}Sb$ SL only *slightly* exceeds that of the $InAs/InAs_{1-x}Sb_x$ SL so that the real distinction between choice of materials will come from practical, growth-related variations.[17] With the major improvements in molecular beam epitaxy (MBE) and metalorganic chemical vapor deposition (MOCVD) technologies in the last couple of decades, it is an ideal time to investigate the $InAs/InAs_{1-x}Sb_x$ SL system experimentally. MOCVD technology compared to MBE has very high throughput, which is good for mass production, and thus is worth investigating despite it being a challenge to grow high-quality antimonides compared to MBE at present.

Photoluminescence (PL) near 10 μm has been reported for a 4 μm thick $InAs_{0.62}Sb_{0.38}/InAs_{0.54}Sb_{0.46}$ SL grown by MBE on GaSb using a graded SL for a strain-balancing buffer layer,[19] a 2 μm thick $InAs/InAs_{0.61}Sb_{0.39}$ SL grown by MBE on GaAs with an $InAs_{0.80}Sb_{0.20}$ buffer,[20,21] and most recently a 6-period $InAs/InAs_{0.733}Sb_{0.267}$ SL grown by MOCVD on an $InAs_{0.91}Sb_{0.09}$ buffer on GaSb.[22] To be suitable for infrared detectors, thick, high-quality materials are necessary, which can be achieved via strain-balancing the individual SL layers on the substrate to avoid misfit dislocations. GaSb is the ideal substrate for strain-balancing InAs/InAsSb SLs due to its lattice constant being between that of the two layers, eliminating the need for complicated metamorphic buffer layers and thus simplifying the growth process.[18] As the Sb concentration in the $InAs_{1-x}Sb_x$ layer increases, the strain of the layer on GaSb increases making the growth more difficult; but reaching LWIR wavelengths (8–12 μm) requires higher Sb concentrations to maintain larger electron-hole wave function overlaps for stronger absorption. We report here a detailed study of the structural and optical properties of thick (50 or 100 periods), $InAs/InAs_{1-x}Sb_x$ type-II SLs with varying Sb compositions (x = 0.22, 0.23, 0.37) grown by MOCVD on GaSb substrates.

To design the $InAs/InAs_{1-x}Sb_x$ SL transition wavelengths for infrared applications, the band edge alignment with strain effects was first calculated. Then strain-balanced thicknesses for the InAs and $InAs_{1-x}Sb_x$ layers strained on GaSb were determined using the thickness-weighted method to achieve zero average strain in the growth direction. Finally, the Kronig-Penney model was solved to obtain the

[a)]Electronic mail: yhzhang@asu.edu.

 © 2011 American Institute of Physics

This article is copyrighted as indicated in the article. Reuse of AIP content is subject to the terms at: http://scitation.aip.org/termsconditions. Downloaded to IP: 209.147.144.24 On: Thu, 05 Feb 2015 17:49:47

TABLE I. Structural details for the superlattices studied in this work.

Sample	x ± 1(%)	Thickness(nm)		Number of periods	Calculated E^g at 0 K(meV)	Photoresponse onset at 10 K(meV)	PL peak position at 6 K(meV)
		InAs	InAsSb				
A: 3-2006	22	7.0	3.3	100	224	177	185
B: 3-2008	23	7.0	2.3	50	250	214	213
C: 3-2009	37	7.0	2.0	50	171	130	–

energy states and wave functions, from which the lowest energy transition and the wave function overlaps were calculated. Table I displays the calculated transition energies.

The $InAs/InAs_{1-x}Sb_x$ SLs were grown by MOCVD at 500 °C on 2 in. (100) n-GaSb substrates following deposition of a 50 nm GaSb buffer layer using growth conditions reported previously.[18] The prior Sb compositions of the sample structures were based on growth calibrations[18] and are different from the details shown in Table I, which were determined by analysis of x-ray diffraction (XRD) measurements. The layer thicknesses are still assumed to be the same values from the growth calibrations. The (004) and (224) $\omega-2\theta$ coupled high-resolution XRD patterns were recorded using a PANalytical X'Pert Pro MRD. The simulation results closely agree with the experimental data, as shown in Fig. 1 for the (004) patterns. Sample A shows intense satellite peaks with narrow full width at half maximum (FWHMs) of less than 100 arc sec, indicating the high degree of crystallinity and uniform periodicity of this SL structure. Some variation in the $InAs_{1-x}Sb_x$ composition, however, is evident from the peaks' shapes. The simulation used varying Sb compositions for different portions of the 100 periods. The most intense SL satellite peaks correspond to an average $x = 0.22$ in the $InAs_{1-x}Sb_x$ layer for the majority of the periods, while the broader, less intense, periodic shoulder peaks are simulated well with just a few periods containing $x = 0.35$. The average relaxation of the SL was 74%, as determined from (224) $\omega-2\theta$ coupled scans. The satellite peaks of sample B are broader than those of sample A, and the simulated pattern of sample B in Fig. 1 uses 83% relaxation and $x = 0.23$ derived from (224) $\omega-2\theta$ coupled scans. The XRD patterns of sample C exhibited 100% relaxation.

Specimens for cross-sectional transmission electron microscopy (TEM) observation were prepared by standard mechanical polishing, dimpling, and argon-ion-milling at reduced energy (2–2.5 keV), with the sample held at liquid-nitrogen temperature to minimize thermal and ion-beam damage. Figure 2 shows a cross-sectional TEM image of sample A, which confirms the very high crystallinity of this specimen. In contrast, samples B and C showed the presence of considerable growth defects, especially {111}-type stacking faults, originating at either the substrate/buffer interface or the buffer/SL interface, and propagating well into the SL region. These defects presumably contribute significantly towards broadening the FWHM of the XRD satellite peaks.

The low temperature PL spectra for samples A and B are shown in Fig. 3. The data were acquired with a double-modulation Fourier transform infrared spectrometer setup to suppress the background 300 K blackbody radiation noise near 10 μm. However, the increasing background noise is still visible in the spectra near the MCT detector cutoff at 12 μm. The 532 nm pumping laser was modulated at 60 kHz. Using a Lorentzian fit to the data, the peak position, intensity, and FWHM for sample A are 185 meV, 822 a.u., and 20 meV and for sample B are 213 meV, 872 a.u., and 32 meV. The PL intensity is comparable for both samples measured under the same conditions, but the FWHM of sample B's spectrum is 60% larger than that of sample A, due to the higher density of defects, as deduced from the TEM, and the higher degree of relaxation in sample B.

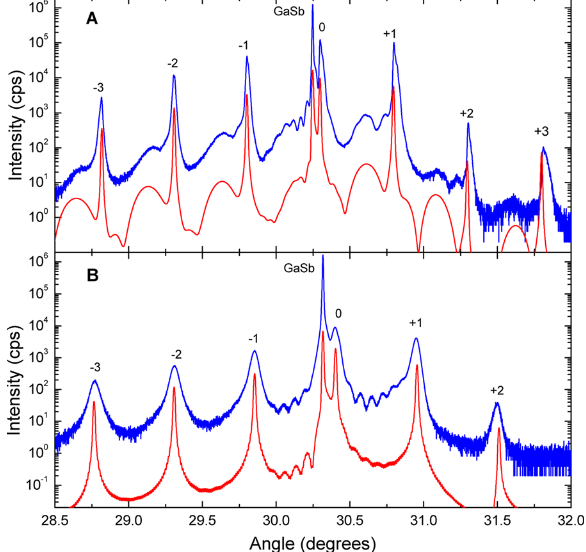

FIG. 1. (Color online) High-resolution (004) XRD patterns and simulations (offset below each measurement) for samples A and B.

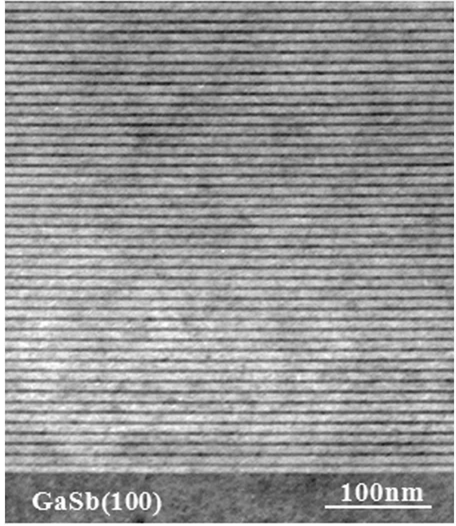

FIG. 2. Cross-sectional transmission electron micrograph of sample A demonstrating the excellent crystallinity of the InAs/InAsSb superlattice grown on a GaSb (100) substrate.

This article is copyrighted as indicated in the article. Reuse of AIP content is subject to the terms at: http://scitation.aip.org/termsconditions. Downloaded to IP: 209.147.144.24 On: Thu, 05 Feb 2015 17:49:47

FIG. 3. (Color online) Photoluminescence spectra at 6 K for samples A and B. The inset shows the type-II band alignment between InAs and $InAs_{1-x}Sb_x$.

The spectral photoconductivity of all three samples was measured using a BioRad FTIR at increasing temperatures from 10 K until the signal disappeared—up to 250 K for sample A, 77 K for sample B, and just at 10 K for sample C. A bias current of 4 mA for sample A and 0.5 mA for sample B was applied at indium contacts on the top surface of the samples. The individual photoconductivity signals were corrected for the background with a reference spectrum. Figure 4 shows the temperature-dependent spectral photoresponse for sample A with a strong response up to 200 K (onset at 8.6 μm) and sample B with response up to 60 K (onset at 5.9 μm). To determine the onset of photoresponse, a linear fit was made to the steep segment of the response as it approached zero, and the x-intercept of the linear function was taken as the photoresponse onset.

Table I shows the comparison of the PL peak position and the photoresponse onset. They agree very well for sample B. For sample A, the PL peak position is higher in energy than the absorption onset, due to the band filling effect caused by the relatively high pump power intensity. Taking the SL relaxation into account, the calculated values follow the same trend as the measured values, although there is a discrepancy due to the measurement uncertainty of x ($\pm$1%) and the layer thicknesses.

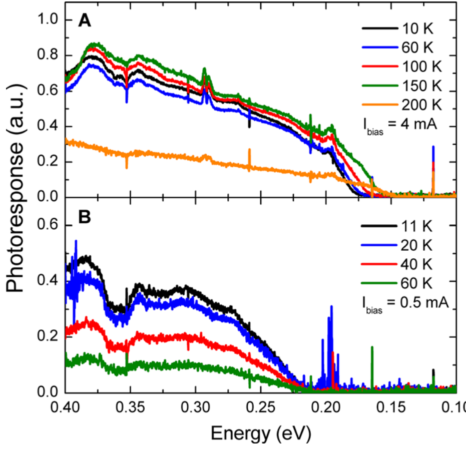

FIG. 4. (Color online) The temperature-dependent spectral photoresponse of sample A, showing strong signals up to 200 K and out to 8.6 μm (145 meV), and sample B, showing signals up to only 60 K and out to 5.9 μm (210 meV).

In summary, $InAs/InAs_{1-x}Sb_x$ SLs grown by MOCVD were studied as an alternative material to HgCdTe for infrared photodetectors. Strong, narrow satellite peaks in the x-ray diffraction pattern and minimal defects in the transmission electron micrograph revealed the excellent structural properties of this strain-balanced $InAs/InAs_{1-x}Sb_x$ SL. In addition, intense photoluminescence spectra and photoconductivity spectral responses up to 200 K at 8.6 μm were observed. The structural properties plus the strong optical responses, despite relaxation occurring, warrant further investigation of these superlattice materials grown by MOCVD for infrared photodetector applications.

The authors are grateful for the support of ARO MURI programs W911NF-06-1-0353 and W911NF-10-1-0524 and an AFOSR Grant (FA9550-10-1-0129). Many experiments were performed at AFRL/RXPS with the support of G. Brown and B. Ullrich. E.H.S. appreciates the DOD SMART and SFAz scholarships. R.D.D. is thankful for the support of the Steve W. Chaddick Endowed Chair in Electro-Optics and the Georgia Research Alliance.

[1]L. Esaki and R. Tsu, IBM J. Res. Dev. **14**, 61 (1970).
[2]G. Sai-Halasz, R. Tsu, and L. Esaki, Appl. Phys. Lett. **30**, 651 (1977).
[3]H. Sakaki, L. L. Chang, G. Sai-Halasz, C. A. Chang, and L. Esaki, Solid State Commun. **26**, 589 (1978).
[4]G. C. Osbourn, J. Vac. Sci. Technol. B **2**, 176 (1984).
[5]J. N. Schulman and T. C. McGill, Appl. Phys. Lett. **34**, 663 (1979).
[6]G. C. Osbourn, L. R. Dawson, R. M. Biefeld, T. E. Zipperian, I. J. Fritz, and B. L. Doyle, J. Vac. Sci. Technol. A **5**, 3150 (1987).
[7]J. Bajaj, G. Sullivan, D. Lee, E. Aifer, and M. Razeghi, Proc. SPIE – Int. Soc. Opt. Eng. **6542**, 65420 (2007).
[8]D. L. Smith, T. C. McGill, and J. N. Schulman, Appl. Phys. Lett. **43**, 180 (1983).
[9]D. H. Chow, R. H. Miles, J. N. Schulman, D. A. Collins, and T. C. McGill, Semicond. Sci. Tech. **6**, 47 (1991).
[10]S. D. Gunapala, D. Z. Ting, C. J. Hill, J. Nguyen, A. Soibel, S. B. Rafol, S. A. Keo, J. M. Mumolo, M. C. Lee, J. K. Liu, and A. Liao, 23rd Annual Meeting of the IEEE Photonics Society, Denver, Colorado, 7–11 November 2010, p. 637.
[11]M. Sundaram, A. Reisinger, R. Dennis, K. Patnaude, D. Burrows, J. Bundas, K. Beech, and R. Faska, Proc. SPIE – Int. Soc. Opt. Eng. **7660**, 76601P (2010).
[12]M. Razeghi, D. Hoffman, B.-M. Nguyen, P.-Y. Delaunay, E. K.-W. Huang, M. Z. Tidrow, and V. Nathan, Proc. IEEE **97**, 1056 (2009).
[13]F. Rutz, R. Rehm, J. Schmitz, J. Fleissner, M. Walther, R. Scheibner, and J. Ziegler, Proc. SPIE – Int. Soc. Opt. Eng. **7298**, 72981R (2009).
[14]I. Vurgaftman, C. L. Canedy, E. M. Jackson, J. A. Nolde, C. A. Affouda, E. H. Aifer, J. R. Meyer, A. Hood, A. J. Evans, and W. T. Tennant, Opt. Eng. **50**, 061007 (2011).
[15]D. Donetsky, G. Belenky, S. Svensson, and S. Suchalkin, Appl. Phys. Lett. **97**, 052108 (2010).
[16]Y.-H. Zhang, Appl. Phys. Lett. **66**, 118 (1995).
[17]C. H. Grein, M. E. Flatte, and H. Ehrenreich, in *Proceedings on the Third International Symposium on Long Wavelength Infrared Detectors and Arrays: Physics and Applications III*, Chicago, Illinois, 8-13 Oct. 1995, p. 211.
[18]Y. Huang, J.-H. Ryou, R. D. Dupuis, V. R. D'Costa, E. H. Steenbergen, J. Fan, Y.-H. Zhang, A. Petschke, M. Mandl, and S.-L. Chuang, J. Cryst. Growth **314**, 92 (2011).
[19]S. R. Kurtz, L. R. Dawson, R. M. Biefeld, D. M. Follstaedt, and B. L. Doyle, Phys. Rev. B **46**, 1909 (1992).
[20]M. J. Pullin, P. J. P. Tang, S. J. Chung, C. C. Phillips, R. A. Stradling, A. G. Norman, Y. B. Li, and L. Hart, in *Proceedings of Seventh International Conference on Narrow Gap Semiconductors*, Santa Fe, New Mexico, 8-12 Jan. 1995, p. 8.
[21]Y. B. Li, D. J. Bain, L. Hart, M. Livingstone, C. M. Ciesla, M. J. Pullin, P. J. P. Tang, W. T. Yuen, I. Galbraith, C. C. Phillips, C. R. Pidgeon, and R. A. Stadling, Phys. Rev. B **55**, 4589 (1997).
[22]D. Lackner, O. J. Pitts, M. Steger, A. Yang, M. L. W. Thewalt, and S. P. Watkins, Appl. Phys. Lett. **95**, 081906 (2009).

This article is copyrighted as indicated in the article. Reuse of AIP content is subject to the terms at: http://scitation.aip.org/termsconditions. Downloaded to IP: 209.147.144.24 On: Thu, 05 Feb 2015 17:49:47